Hyperkalemic Periodic Paralysis and Permanent Weakness: 3-T MR Imaging Depicts Intracellular ^{23}Na Overload—Initial Results[1]

Erick Amarteifio, MD
Armin M. Nagel, PhD
Marc-André Weber, MD, MSc
Karin Jurkat-Rott, PhD
Frank Lehmann-Horn, MD, PhD

Purpose: To assess whether myoplasmic ionic sodium (Na^+) is increased in muscles of patients with hyperkalemic periodic paralysis (HyperPP) with 3-T sodium 23 (^{23}Na) magnetic resonance (MR) imaging and to evaluate the effect of medical treatment on sodium-induced muscle edema.

Materials and Methods: This study received institutional review board approval; written informed consent was obtained. Proton (hydrogen 1 [^{1}H]) and ^{23}Na MR of both calves were performed in 12 patients with HyperPP (mean age, 48 years ± 14 [standard deviation]) and 12 healthy volunteers (mean age, 38 years ± 12) before and after provocation (unilateral cooling, one calf). ^{23}Na MR included spin-density, T1-weighted, and inversion-recovery (IR) sequences. Total sodium concentration and normalized signal intensities (SIs) were evaluated within regions of interest (ROIs). Muscle strength was measured with the British Medical Research Council (MRC) grading scale. Five patients underwent follow-up MR after diuretic treatment.

Results: During rest, mean myoplasmic Na^+ concentration was significantly higher in HyperPP with permanent weakness (40.7 μmol/g ± 3.9) compared with HyperPP with transient weakness (31.3 μmol/g ± 4.8) (P = .004). Mean SI in ^{23}Na IR MR was significantly higher in HyperPP with permanent weakness (0.83 ± 0.04; median MRC, grade 4; range, 3–5) compared with HyperPP without permanent weakness (0.67 ± 0.05; median MRC, grade 5; range, 4–5) (P = .002). Provocation reduced muscle strength in HyperPP (before provocation, median MRC, 5; range, 3–5; after provocation, median MRC, 3; range, 1–4) and increased SI in ^{23}Na IR from 0.75 ± 0.09 to 0.86 ± 0.10 (P = .004). Spin-density and T1-weighted sequences were less sensitive, particularly to cold-induced Na^+ changes. ^{23}Na IR SI remained unchanged in volunteers (0.53 ± 0.06 before and 0.54 ± 0.06 after provocation, P = .3). Therapy reduced mean SI in ^{23}Na IR sequence from 0.85 ± 0.04 to 0.64 ± 0.11.

Conclusion: ^{23}Na MR imaging depicts increased myoplasmic Na^+ in HyperPP with permanent weakness. Na^+ overload may cause muscle degeneration developing with age. ^{23}Na MR imaging may have potential to aid monitoring of medical treatment that reduces this overload.

[1] From the Department of Diagnostic and Interventional Radiology, University Hospital of Heidelberg, Im Neuenheimer Feld 110, D-69120 Heidelberg, Germany (E.A., M.A.W.); Department of Medical Physics in Radiology (A.M.N.) and Radiology (E.A., M.A.W.), German Cancer Research Center, Heidelberg, Germany; and Department of Neurophysiology, Ulm University, Ulm, Germany (K.J., F.L.). From the 2009 RSNA Annual Meeting. Received May 12, 2011; revision requested July 2; final revision received December 16; accepted December 29; final version accepted January 6, 2012. **Address correspondence to** E.A. (for MR imaging, e-mail: *erick.amarteifio@med.uni-heidelberg.de*) or F.L. (for hyperkalemic periodic analysis, e-mail: *frank.lehmann-horn@uni-uhm.de*).

Hyperkalemic periodic paralysis (HyperPP) is a dominantly inherited muscle disease characterized by attacks of flaccid weakness and interictal myotonia (1). The incidence of HyperPP is approximately one per 200 000 persons, and its penetrance within the population is high with more than 90% (2). HyperPP is a channelopathy caused by mutations in the *SCN4A* gene coding for the Nav1.4 muscle sodium channel (3–5). The disease includes both hyper- and hypoexcitability of muscle fibers, frequently in the same patient at different times (6). The flaccid muscle weakness (paralysis) is typically triggered by ingestion of potassium-rich foods or rest following physical strain (7). Some patients require medication, including hydrochlorothiazide (Hct Hexal; Hexal, Holzkirchen, Germany) or acetazolamide (Diamox; Goldshield Pharmac, Croydon, England) (8).

The underlying sodium ion (Na^+) channel mutations destabilize the inactivated channel state. This results in a persistent current, which could lead to Na^+ accumulation in the muscle (9). Until now, Na^+ accumulation has been described in HyperPP fibers exposed to increased extracellular potassium ion (K^+) concentration in vitro by using Na^+-sensitive microelectrodes (10). Also Na^+ accumulation during weakness episodes has been described in vivo after provocation with specific triggers by using sodium 23 (^{23}Na) magnetic resonance (MR) imaging (11).

Recent studies have shown the potential of ^{23}Na MR imaging for quantification of total sodium amount in human muscle (12). A central problem in ^{23}Na MR imaging is that the signal emitted from muscle tissue is roughly 50 000 times smaller than the signal received from standard proton (hydrogen 1 [^{1}H]) MR imaging (13). The short T2 relaxation time of ^{23}Na in (muscular) tissue causes a low signal-to-noise ratio when conventional measuring times are used. This is still the case when newer density-adapted three-dimensional radial acquisition techniques are used to improve the results (14,15). A further challenge with any imaging method is the precise differentiation between intra- and extracellular ^{23}Na. With T1-weighted ^{23}Na MR imaging sequences, a muscular Na^+ accumulation in muscular channelopathies can be visualized (16), but a measure of intra- and extracellular Na^+ amounts is not provided. Shift reagents would enable a clear separation between intra- and extracellular Na^+, but they cannot be administered to humans because of their toxicity (17). Other techniques do not allow a separate measurement of intra- and extracellular Na^+.

The extracellular Na^+ concentration is about 10 times higher than the intracellular Na^+ concentration, which allows a rough estimation of intracellular sodium content changes by measuring the total Na^+ concentration (18). Meanwhile, it is possible to provide a partial suppression of signal from sodium ions in the extracellular milieu (eg, cerebrospinal fluid, blood) by using an inversion-recovery (IR) ^{23}Na MR imaging sequence (19). Furthermore, results from investigations of patients with muscular channelopathies indicate that an IR preparation allows for a weighting toward intracellular sodium (20). In an analysis on paramyotonia, an allelic disorder, noninvasive ^{23}Na MR imaging techniques at 1.5-T for detecting changes of the Na^+ signal in muscular tissue after provocation were implemented (16). Also, these techniques have been successfully refined to aid qualitative visualization of changes of the muscular Na^+ amount in patients with hypokalemic periodic paralysis in a state of severe permanent weakness (9,20). The studies mentioned above present important findings on channelopathies. However, to our knowledge, the researchers in none of the published studies noninvasively analyzed the myoplasmic sodium amount in patients with various types of HyperPP. In the current study, IR ^{23}Na MR imaging sequences were included to allow for a reduction of signal emitted by blood vessels and muscular edema. The rationale was a better visualization of intracellular sodium content changes that are primarily responsible for muscle weakness.

Thus, the aim of the current study was to assess whether the myoplasmic Na^+ in patients with HyperPP with permanent weakness is increased during rest or after provocation by using 3-T

Advances in Knowledge

- The implementation of a ^{23}Na MR imaging inversion-recovery sequence allowed for a weighting toward intracellular ^{23}Na with a high sensitivity.
- With this technique, a markedly increased intracellular sodium concentration of resting skeletal muscle was detected in patients with hyperkalemic periodic paralysis (HyperPP) with permanent weakness.
- Acetazolamide and hydrochlorothiazide decreased the intracellular sodium level and increased muscle strength.

Implication for Patient Care

- Increased myoplasmic sodium acts as an indicator of permanent muscle weakness in HyperPP and precedes fatty muscle degeneration.

Published online before print
10.1148/radiol.12110980 **Content code:** MK

Radiology 2012; 264:154–163

Abbreviations:
HyperPP = hyperkalemic periodic paralysis
IR = inversion recovery
MRC = British Medical Research Council
ROI = region of interest
SI = signal intensity
STIR = short inversion time inversion recovery

Author contributions:
Guarantors of integrity of entire study, E.A., M.A.W.; study concepts/study design or data acquisition or data analysis/interpretation, all authors; manuscript drafting or manuscript revision for important intellectual content, all authors; approval of final version of submitted manuscript, all authors; literature research, E.A., F.L.; clinical studies, E.A., A.M.N., M.A.W., F.L.; experimental studies, E.A., A.M.N., K.J., F.L.; statistical analysis, E.A., F.L.; and manuscript editing, all authors

Potential conflicts of interest are listed at the end of this article.

^{23}Na MR imaging. Moreover, the effect of medical treatment was evaluated with ^{23}Na MR imaging.

Materials and Methods

Patients and Volunteers

The study was approved by the institutional review boards of Heidelberg University (Heidelberg, Germany) and Ulm University (Ulm, Germany) and conducted according to the Declaration of Helsinki. Written informed consent was obtained from all volunteers and patients after the nature of the examination and its purpose had been fully explained. Twelve patients, four women (mean age, 43 years ± 16 [standard deviation]) and eight men (mean age, 50 years ± 12) with genetically proved HyperPP were included in this study (all patients, mean age, 48 years ± 14). Six patients had permanent muscle weakness, and six patients had episodic muscle weakness. The control group included 12 healthy volunteers, five women (mean age, 33 years ± 9) and seven men (mean age, 41 years ± 12) without any evidence of muscular or cardiovascular disorders (all patients, mean age, 38 years ± 12), with $P = .06$. All volunteers had full muscle strength at physical examination and had normal findings at ^{1}H MR imaging. All subjects were examined with MR imaging during a period from February 2009 to October 2010.

Patient Examination Protocol

^{1}H and ^{23}Na MR imaging were performed on both calves before provocation and after provocation of one calf. The provocation was accomplished by cooling with ice-water bags (32°F; 273 K) wrapped around the nondominant calf for 25 minutes while the subject rested on a stretcher. Directly after cooling, the subjects were instructed to perform dorsiflexion with their feet against the examiner's resistance 30 times, as proposed by the standardized British Medical Research Council (MRC) grading scale. Subsequently, they had to stand and shift their weight alternately on their heels and on tiptoes 30 times. In five patients, follow-up MR imaging was performed after treatment with acetazolamide or hydrochlorothiazide lasting several weeks.

Muscle Strength Grading

The muscle strength was quantified with the aid of the nonlinear grading system defined by the MRC, as follows: grade 0, complete paralysis; grade 1, minimal contraction; grade 2, active movement with gravity eliminated; grade 3, weak contraction against gravity; grade 4, active movement against gravity and resistance; and grade 5, normal strength (21). Examination of the calves consisted of strength testing of dorsiflexion, plantar flexion, toe dorsiflexion, and toe plantar flexion both of the reference leg and the leg with provocation. Muscular strength was evaluated before and immediately after provocation, as well as 45 minutes after provocation. Muscle strength was quantified by two authors (M.A.W., a physician with 11 years of experience in radiology with a focus on musculoskeletal MR imaging and 6 years of experience in neurology, and E.A., a radiologist with 3 years of experience in musculoskeletal MR imaging) in consensus.

^{23}Na MR Imaging Technique

MR imaging was performed with a 3-T clinical MR system (Magnetom Trio; Siemens Medical Solutions, Erlangen, Germany) by using specific hardware for broadband spectroscopy and a Comunità Europea–certified double-resonant birdcage coil (32.59 MHz/123.2 MHz; Rapid Biomed, Würzburg, Germany) for the ^{23}Na and ^{1}H measurements.

^{23}Na MR Imaging Protocol

The ^{23}Na signal decays in a biexponential manner (fast T2, 0.5–3 msec; slow T2, 15–30 msec). A very-short echo time, less than 0.5 msec, is required to receive the total sodium signal (22). Three ^{23}Na pulse sequences based on a density-adapted three-dimensional radial sequence were used. To visualize the local Na^+ concentration, T1 and T2* weighting in the gradient-echo data sets was minimized by using a short echo time (0.2 msec) and a long repetition time (100 msec; flip angle, 90°; voxel size, 5 × 5 × 5 mm^3; acquisition time, 8 minutes 20 seconds).

Two reference phantoms (length, 3.9 inches [9.9 cm]; width, 2.4 inches [6.1 cm]; volume, 285 mL) were placed on the calves of the subjects. The first phantom was filled with 51.3 mmol/L saline solution to represent Na^+ with long relaxation times (eg, comparable to Na^+ in extracellular edema). The second phantom contained 51.3 mmol/L Na^+ bounded with 5% agarose gel to represent Na^+ with T1 relaxation times close to those of healthy muscle tissue. Because the Na^+ concentration of present reference tubes was known (51.3 mmol/L; ie, 0.3% NaCl solution), the average Na^+ concentration of muscular tissue was calculated by using linear extrapolation and then converted in micromoles per gram of wet-tissue weight by multiplying by the specific gravity of muscle (23). Then a ^{23}Na T1 image contrast was used to get a higher weighting of Na^+ ions with short T1 relaxation time (repetition time msec/echo time msec, 6/0.25; flip angle, 40°; voxel size, 5 × 5 × 5 mm^3; acquisition time, 5 minutes 36 seconds). Last, a ^{23}Na IR sequence was applied to reduce the ^{23}Na signal received from vasogenic edema, as well as the ^{23}Na signal received from the extracellular space, to achieve a direct weighting of the intracellular Na^+ amount (repetition time msec/echo time msec/inversion time msec, 124/0.3/34; voxel size, 6 × 6 × 6 mm^3; acquisition time, 10 minutes 20 seconds) (20). For all sequences, very-short echoes were applied to minimize T2* weighting.

Analysis of the ^{23}Na and ^{1}H MR Imaging Data

The image analysis was performed at a picture archiving and communication system (Centricity, version 3.0.4; GE Healthcare Integrated IT Solutions, Barrington, Ill) that allowed for a direct comparison and coregistration of anatomic and functional data sets on two large-screen high-resolution monitors. All MR examinations were jointly randomized, and identifying parameters such as the patient's name were removed before

region of interest (ROI) analysis. With the objective of quantifying the ^{23}Na MR signal at rest, as well as the signal alteration on the ^{23}Na MR images after provocation of the nondominant calf, the three-dimensional radial images were analyzed by using the ROI. ROIs were positioned on the muscles of the subject's calf by two radiologists (E.A. and M.A.W.) in consensus. For exact positioning, the ^{1}H MR images were used as reference (Fig 1). When distinct lipomatous degeneration of certain calf muscles was observed on ^{1}H MR images, the ROIs were positioned in an area of more intact muscle. To reduce measurement error and variability, the ROIs were placed in at least 10 different sections of each calf. The average of the values was then calculated. Supplementary ROIs were placed on two reference phantoms. In addition, the ROIs and reference tubes were placed to the center as closely as possible to avoid measurement errors caused by coil field inhomogeneity. The signal intensities (SIs) on the ^{23}Na MR images were normalized to the 51.3 mmol/L saline solution phantoms by dividing the values of the ROIs positioned on the soleus muscles by the values of the ROIs on the reference phantoms. Hereby, interindividual and intraindividual comparisons were permitted. The SIs for both calves of the subject were analyzed before and after provocation. Observed enhancement of the SI was considered to mirror changes in muscular Na^+ concentration. The resulting percentage difference (SI%) of normalized muscular ^{23}Na imaging SI before (SI_{pre}) and after provocation (SI_{post}) was evaluated with assistance of the following equation (11): $\Delta SI\% = (SI_{post} - SI_{pre})/SI_{pre} \cdot 100$.

In addition, ^{1}H MR imaging was performed to detect muscular pathologic findings, such as edematous and lipomatous changes, of the calves of the patients and volunteers. A transverse T1-weighted turbo spin-echo sequence (700/10; matrix, 275 × 448; section thickness, 3 mm) and a transverse fluid-weighted short inversion time inversion-recovery (STIR) sequence (6920/65; matrix, 176 × 320; section thickness, 4 mm) were included in the ^{1}H MR imaging protocol. Image interpretation was performed by two radiologists (M.A.W. and E.A.), who were blinded to the clinical data, in consensus. Areas of localized hyperintensity on T2-weighted and fat-saturated MR images were defined as muscle edema. Areas of intensity equivalent to the signal received from subcutaneous fat on T1- and T2-weighted MR images were interpreted as fatty infiltration caused by chronic myopathy. Presence of these findings was scored in a binary fashion.

Figure 1

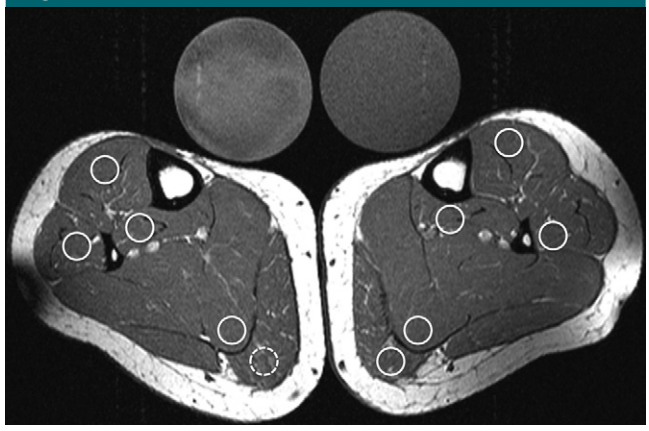

Figure 1: Sample ROI placement in a 34-year-old woman with HyperPP and episodic weakness. Transverse ^{1}H MR images (700/10) of the calves show discrete fatty atrophy within the right gastrocnemius muscle (dotted-line circle).

The muscle cross-sectional area was assessed qualitatively by two radiologists (M.A.W. and E.A.) in consensus. This was done to elucidate muscle atrophy by using the opposite calf or other muscle groups for comparison.

Besides the qualitative image analysis, the lipomatous changes of the soleus muscle were quantified by assessing the ratio of SI of muscle to SI of subcutaneous fat tissue by using an ROI analysis according to Bachmann et al (24). ROIs were placed on T1-weighted images of the same sections used for ^{23}Na MR image analysis. Attention was paid by the assessor to avoid ROI placement in those regions of the calves affected by signal inhomogeneities. The mean of the ratios of SI of muscle and subcutaneous fat tissue was used for statistical analysis. Moreover, edematous changes of the soleus muscle were also quantified with ROI analysis by using the saline solution phantom (51.3 mmol/L; ie, 0.3% NaCl solution) to normalize the signal.

Detection of Channel Mutation

Blood preserved with ethylenediaminetetraacetic acid (20 mL each) was obtained for *SCN4A* mutation analysis. Mutation screening was performed by using polymerase chain reaction amplification of *SCN4A* exons 13, 22, and 24. Polymerase chain reaction products were loaded on a 2% agarose gel and were stained with ethidium bromide, and the band was cut out under ultraviolet light. Bands were purified by using the DNA sequencing kit (Amersham Pharmacia Biotech, Piscataway, NY) and were cycle-sequenced with 1 pmol of primer using the dye terminator kit (Applied Biosystems, Foster City, Calif). Sequencing was performed on 6% denaturing polyacrylamide gels in an automated DNA sequencer (ABI 377 HT; Applied Biosystems, Foster City, Calif). All sequences with base exchanges were verified by reverse sequencing of a new polymerase chain reaction product of the same DNA sample.

Statistical Analysis

All data management, statistical analyses, and the construction of the box and whisker plots were performed by using software (SAS, version 9.2; SAS, Cary, NC). Nonparametric exact Wilcoxon *U* tests (two sided) for independent data and

Figure 2

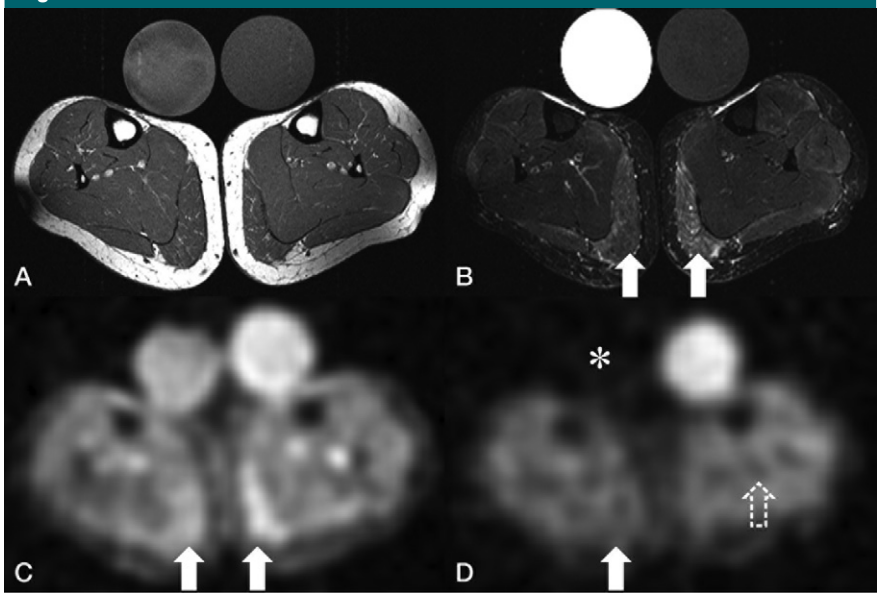

Figure 2: Transverse MR images of both calves in a 47-year-old woman with genetically confirmed HyperPP. While, *A,* T1-weighted ^{1}H images (700/10) of both calves show normal findings, *B,* fat-saturated T2-weighted STIR ^{1}H images (6920/65) reveal muscular edema of both gastrocnemius muscles (arrows, also on *C*). *C,* ^{23}Na T1-weighted MR images (6/0.25) reveal an elevated signal in both gastrocnemius muscles. *D,* On the ^{23}Na IR images (124/0.3/34), the signal of vasogenic edema (white arrow) and vessels (open arrow) is reduced. Suppressed signal was observed in the reference tube containing 0.3% saline solution (*).

Figure 3

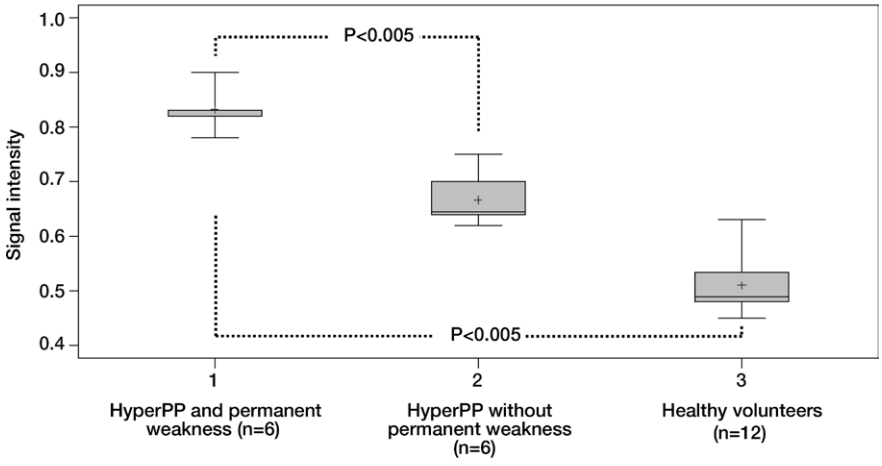

Figure 3: Graphs show SI after ROI placement on MR images generated with ^{23}Na IR sequence. The patients with HyperPP and permanent weakness (plot *1*) showed a significantly higher SI in comparison with HyperPP patients without permanent weakness (plot *2*). This fact indicates a higher intracellular Na^+ amount in patients with HyperPP and permanent weakness. The healthy volunteers (plot *3*) showed a low SI consistent with normal amount of Na^+ within the muscle cells. + = Mean, horizontal black line = median.

Wilcoxon signed rank tests for dependent data were used to detect differences between patients and control subjects. Results were expressed as mean ± standard deviation for quantitative data and as median and range for the MRC grading scale results. A difference with $P < .05$ was considered significant.

Results

Muscle Strength

Seven patients with HyperPP had paresis of the calf at the time of physical examination. The muscle strength of the patients' calves for foot dorsiflexion and plantar flexion prior to cooling and exercise was median MRC grade 5, with a range of 3–5.

Cooling and exercise caused reduced muscle strength of foot dorsiflexion and plantar flexion in the leg with provocation in 10 of 12 patients with provocation. The muscle strength after provocation was median MRC grade 3, with a range of 1–4. Two patients developed complete paralysis of the upper and lower extremities after the first MR imaging examination even though provocation by cooling was not performed. The muscle strength was median MRC grade 1.

In all patients with HyperPP, muscle strength partially recovered within 45 minutes after provocation. The muscle strength was median MRC grade 4 after recovery, with a range of 2–5.

The healthy volunteers had normal muscle function of both calves at any time before and after provocation. The muscle strength was median MRC grade 5.

^{23}Na IR MR Imaging

With the ^{23}Na IR sequence, suppression of the ^{23}Na signal emitted from areas of edema and blood vessels was achieved (Fig 2). Prior to provocation, higher mean SIs were observed in the HyperPP patients with permanent weakness (0.83 ± 0.04; muscle strength, median MRC grade 4; range, 3–5) than in the HyperPP patients without permanent weakness (0.67 ± 0.05; $P = .002$; muscle strength, median MRC grade 5; range, 4–5) or healthy volunteers (0.50 ± 0.06; $P < .005$; muscle strength, median MRC grade 5) (Fig 3).

After cooling and exercise, the mean SI (^{23}Na IR sequence) in the leg with provocation increased in 10 patients with HyperPP (from 0.75 ± 0.09

to 0.86 ± 0.10, P = .004). In the group of patients with permanent weakness, an increase in SI from 0.83 ± 0.04 to 0.93 ± 0.08 was observed after provocation (P < .005). In the group of patients with transient weakness, there was also an increased SI noticed after provocation (from 0.68 ± 0.06 to 0.77 ± 0.06, P < .05).

Two patients did not participate in the provocation, because the rest during the first measurement had already caused a complete (reversible) paralysis (muscle strength, MRC grade 1) of the extremities. In the healthy volunteers, no increase in the ^{23}Na signal (IR sequence) was detectable (from 0.53 ± 0.06 to 0.54 ± 0.06, P = .3), and no weakness occurred (muscle strength, median MRC grade 5 vs grade 5).

T1-weighted ^{23}Na MR Imaging

This method achieved a higher weighting of the intracellular Na^+ amount. HyperPP patients with permanent weakness showed a mean normalized SI of 0.89 ± 0.07 before provocation and 0.87 ± 0.04 after provocation (P > .99) (Fig 4). Those without permanent weakness displayed a mean normalized SI of 0.72 ± 0.10 before provocation and of 0.76 ± 0.11 after provocation (P < .05). In the healthy volunteers, the mean T1-weighted ^{23}Na MR imaging SI was 0.55 ± 0.07 before provocation and 0.55 ± 0.07 after provocation and was thus significantly lower than in the HyperPP patients (P < .005).

Spin-Density ^{23}Na MR Imaging

This method was used to assess the total Na^+ concentration. The HyperPP patients with permanent weakness showed a significantly higher mean Na^+ concentration (40.7 μmol/g ± 3.9) than did those without permanent weakness (31.3 μmol/g ± 4.8, P = .004) and healthy volunteers (24.3 μmol/g ± 3.4, P < .005 for both conditions). In all subject groups, the overall intracellular Na^+ concentration did not change significantly after provocation (Figs 5, 6).

^{1}H MR Imaging

Eight of 12 patients with HyperPP exhibited a hyperintensity of the ^{1}H signal in the T2-weighted STIR sequences prior to provocation. The mean ^{1}H SI ratio of the right gastrocnemius muscle in patients with HyperPP was 0.1 ± 0.05 versus 0.06 ± 0.01 in volunteers (Fig 7).

Seven of 12 HyperPP patients showed high SI ratios within their calf muscles on T1-weighted images. The mean ^{1}H SI ratio of the right gastrocnemius muscle in the HyperPP patients was 0.79 ± 0.57 versus 0.40 ± 0.04 in the volunteers (Fig 8). Patients with HyperPP with permanent weakness presented a high degree of lipomatous changes compared with the group without permanent weakness and healthy volunteers.

A specific pattern of lipomatous changes was noticeable: The highest degree of fatty atrophy was observed in the triceps surae muscle (gastrocnemius muscle with a mean ^{1}H SI ratio on T1-weighted images of 0.79 ± 0.57, followed by the soleus muscle with a ratio of 0.69 ± 0.62). The tibialis anterior muscle showed a mean ^{1}H SI ratio of 0.55 ± 0.58, and the tibialis posterior muscle showed a mean ^{1}H SI ratio of 0.52 ± 0.58. The peroneal muscles (longus, brevis, and tertius) showed concomitantly with the lowest degree of edematous changes also the lowest degree of fatty atrophy, with a mean ^{1}H SI ratio of 0.51 ± 0.51 on T1-weighted images. None of the healthy volunteers showed an increased SI ratio on T1-weighted ^{1}H images (ratio in the right gastrocnemius muscle, 0.40 ± 0.04).

Figure 4

HyperPP Permanent Weakness (n = 5)		HyperPP Episodic Weakness (n = 5)		Volunteers (n = 12)	
Before Provocation	After Provocation	Before Provocation	After Provocation	Before Provocation	After Provocation
0.95	0.92	0.65	0.68	0.61	0.58
0.80	0.85	0.84	0.95	0.55	0.53
0.82	0.87	0.63	0.71	0.62	0.66
0.84	0.82	0.65	0.68	0.52	0.52
0.96	0.90	0.67	0.76	0.56	0.63
				0.46	0.44
				0.48	0.50
				0.48	0.47
				0.69	0.65
				0.55	0.57
				0.50	0.52
				0.53	0.57

Figure 4: Chart shows intraindividual SIs before and after provocation by cooling of the calf measured with T1-weighted ^{23}Na MR imaging. SIs were assessed with ROIs placed within the gastrocnemius muscle.

MR Imaging Examination after Medication

Four patients underwent a repeated ^{1}H and ^{23}Na MR imaging examination after several weeks of continuous medication with either acetazolamide (up to 1000 mg per day) or hydrochlorothiazide (up to 25 mg per day). In these patients the edema within the muscles of the calves decreased during the treatment. Moreover, the treated patients showed a decreased SI in ^{23}Na IR MR imaging sequences (mean, 0.85 ± 0.04 before medication vs 0.64 ± 0.11 after medication) and slightly increased muscle strength for foot dorsiflexion and plantar flexion. The muscle strength was median MRC grade 4, with a range of 4–5, versus median MRC grade 5.

Detection of Channel Mutation

Mutation analysis via polymerase chain reaction amplification of the *SCN4A* exons 13, 22, and 24 showed that 10 of 12 patients were affected by the most frequent T704M mutation (threonine to methionine substitution at codon 704 of the *SCN4A* gene). The two remaining patients were affected by mutation in the same loop connecting segments 5 and 6 of channel domain II.

Discussion

Patients with HyperPP are affected by an incomplete inactivation of muscular Na^+ channels (25). This highly selective

Figure 5

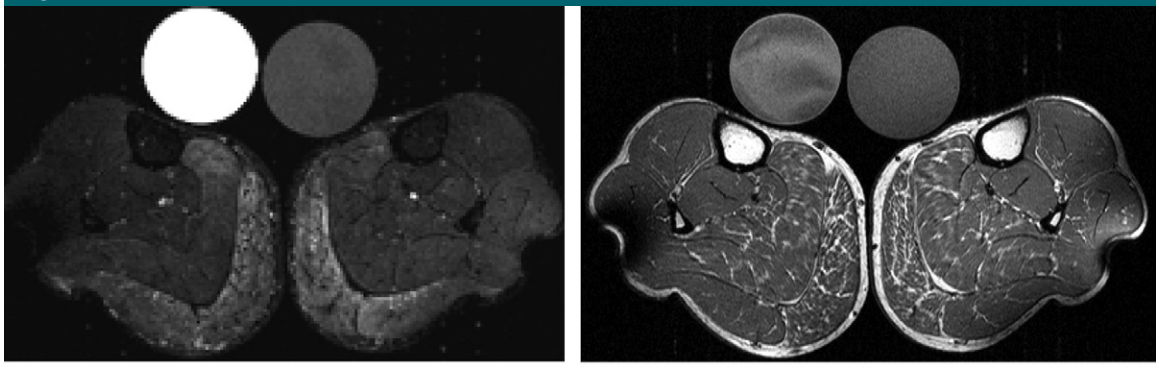

a. b.

Figure 5: Transverse ^{1}H MR images of the calves in a 39-year-old man with HyperPP. **(a)** Fat-saturated T2-weighted STIR images (6920/65) show visualization of edematous changes within the gastrocnemius muscle of both calves. **(b)** T1-weighted images (700/10) demonstrate lipomatous changes of the gastrocnemius muscle, but the soleus muscle is less affected.

Figure 6

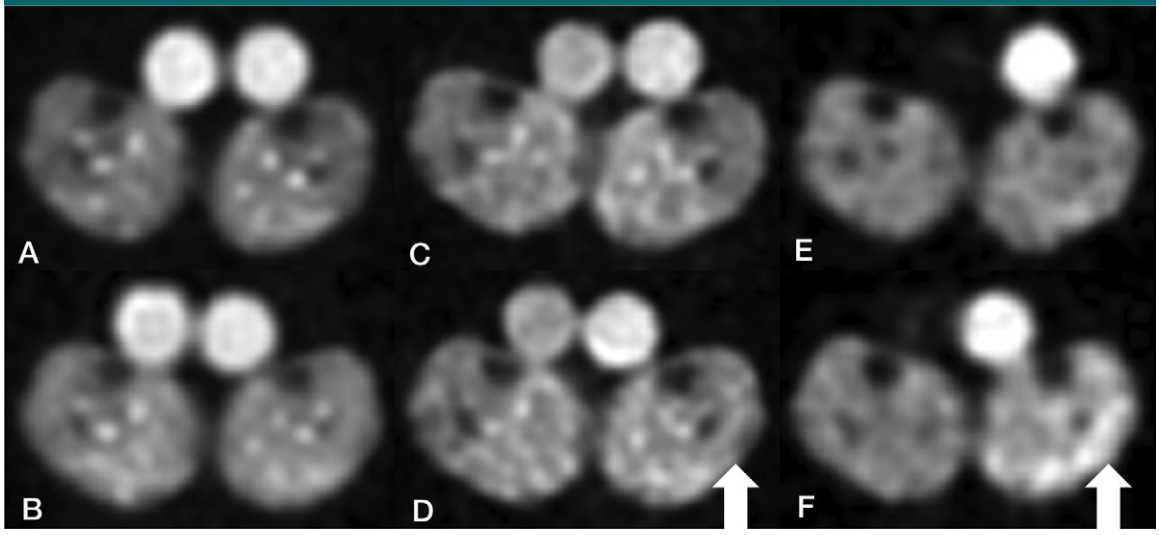

Figure 6: Transverse ^{23}Na MR images of both calves in the same patient as in Figure 5 before and after provocation by cooling of the left calf. No relevant changes of the overall Na^+ concentration, assessed with spin-density image contrast (100/0.2), *A,* before and, *B,* after provocation. ^{23}Na T1-weighted image contrast (6/0.25), *C,* before and, *D,* after provocation. After provocation, a slight signal increase within the left calf is ascertainable (arrow in *D*). ^{23}Na IR images (124/0.3/34), *E,* before and, *F,* after provocation show that the signal increase in the left calf is clearly visible (arrow in *F*), and is probably caused by a pathologic influx of Na^+.

Na^+ leak through the central pore of the mutant channels leads to a permanent inward Na^+ current that is responsible for an ongoing depolarization of the muscle fibers and a transient generation of recurrent action potentials (2), which finally leads to muscle weakness (6).

Our study shows that the implemented ^{23}Na IR sequence is more sensitive to changes of the myoplasmic Na^+ than are ^{23}Na spin-density or ^{23}Na T1 image contrasts (Fig 6). The latter two methods both reflect an average of the intracellular and extracellular Na^+ concentrations. In addition, ^{23}Na MR imaging showed that muscle tissue of patients with HyperPP with permanent muscle weakness features a higher average Na^+ concentration, as well as a higher ^{23}Na IR signal during rest, compared with the patients with HyperPP with transient episodes of weakness. This finding can be attributed to the significantly different ^{23}Na MR imaging findings, although the findings have not been proved through invasive muscle biopsies to measure cation-dependent membrane potential distribution and leaks.

The association of abnormally high myoplasmic Na^+ in HyperPP with the presence of muscle weakness shown in the present work is analogous to findings

Figure 7

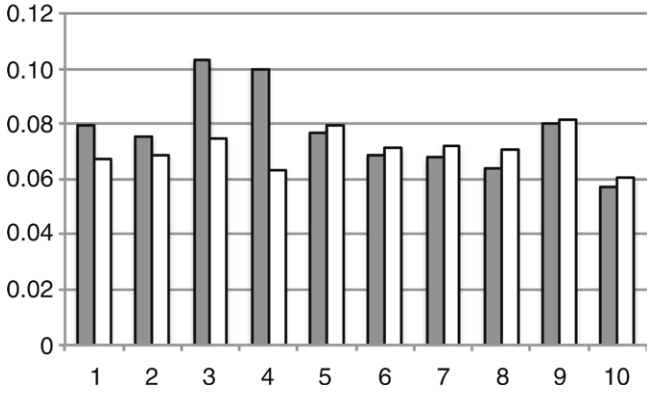

Figure 7: Graph shows SI within the calf muscles of patients with HyperPP (gray bars, $n = 12$) and healthy volunteers (white bars, $n = 12$) measured with ^{1}H STIR MR imaging. The patients with HyperPP showed increased SI within the tibialis anterior muscle and gastrocneumius muscle, indicating edema. *1* = Left tibialis anterior muscle, *2* = right tibialis anterior muscle, *3* = left gastrocnemius muscle, *4* = right gastrocnemius muscle, *5* = left soleus muscle, *6* = right soleus muscle, *7* = left tibialis posterior muscle, *8* = right tibialis posterior muscle, *9* = left peroneal muscle (longus, brevis, and tertius), *10* = right peroneal muscle (longus, brevis, and tertius).

Figure 8

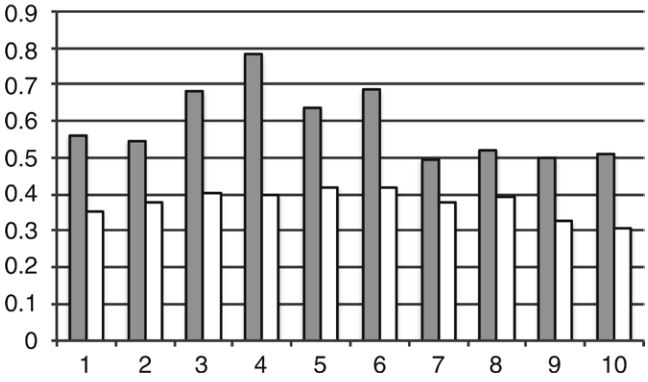

Figure 8: Graph shows SI within the calf muscles of patients with HyperPP (gray bars, $n = 12$) and healthy volunteers (white bars, $n = 12$) measured with T1-weighted ^{1}H MR imaging. The patients with HyperPP showed increased SI within all muscle groups of the calf, indicating fatty atrophy. Keys are the same as for Figure 7.

in hypokalemic periodic paralysis (9). Thus, the permanent weakness seems to be initiated by a gain of function of mutant Na^+ channels. In the long term, the resulting intracellular Na^+ overload disturbs the muscle structure.

This chain of events may be of much more general importance in other muscle disorders, where an abnormal entry of Na^+ into muscle fibers leads to myoplasmic Na^+ overload. This overload, in turn, leads to intracellular and muscular edema (26). The chronic intracellular edema may lead to a loss of muscle cells and finally to fatty atrophy as seen in Duchenne muscular distrophy (27,28). Our findings indicate that the fatty atrophy proceeds with age of the subjects. Younger patients with HyperPP may therefore be expected to exhibit relatively more edematous muscle changes as compared with fatty atrophy.

In both patient groups, a provocation by temporary cooling caused a mean signal increase that was ascertainable with the ^{23}Na IR sequence. There was no significant increase of ^{23}Na signal observed in healthy volunteers either before or after provocation. It may be assumed that the increase of the signal after provocation is caused by a pathologic intracellular Na^+ accumulation.

The ^{23}Na MR imaging protocol included three ^{23}Na pulse sequences based on a density-adjusted three-dimensional radial sequence: With a spin-density image contrast, the total Na^+ concentration was assessed. The overall muscular Na^+ concentration in the volunteers was in agreement with previous published results (12). A ^{23}Na T1 image contrast was performed to achieve a higher weighting of the intracellular Na^+ amount. Last, the ^{23}Na IR sequence was performed to suppress the ^{23}Na signal emitted by extracellular edema and blood vessels and, thus, to allow for a weighting toward intracellular Na^+ that is responsible for membrane depolarization and the subsequent loss of membrane excitability that causes the muscle weakness in patients with HyperPP.

Both ^{23}Na T1 and ^{23}Na spin-density image contrasts reflect an average of the intracellular and extracellular Na^+ concentrations. Because the extracellular Na^+ concentration in tissue water at 140 mmol/L is 10-fold higher compared with the Na^+ concentration in cytosol at 10–15 mmol/L (18), the analysis of intracellular Na^+ is limited when both of the aforementioned sequences are used. However, to understand the disease mechanisms, which cause muscle weakness in patients who have muscular-channel disorders, it seems to be much more important to monitor the changes of intracellular Na^+ concentrations. When physiologic tissue perfusion is assumed, the extracellular amount of sodium will remain constant, and, therefore, changes in the received MR signal will reflect the capacity of the muscle cells to pump out inflowing Na^+ ions against the electrochemical gradient at the cell membrane (18). For this reason, even with ^{23}Na T1 sequences, changes in total Na^+ could be detected after provocation in Na^+ channelopathies (11). Nevertheless, it cannot be excluded that a local increased perfusion generated by reactive hyperemia after provocation (ie, cooling) leads to increased ^{23}Na signal emitted by extracellular Na^+ ions that are circulating in the blood vessels. Moreover, muscular edema and, therefore, an increased amount of extracellular Na^+ may overwhelm the relatively minimal changes on the intracellular level. With ^{23}Na IR MR imaging sequences, a suppression of the ^{23}Na signal emitted by free Na^+ ions (eg, cerebrospinal fluid

or extracellular fluid) is possible, and, therefore, a weighting toward intracellular sodium can be achieved (19,20).

Provocation by cooling caused an increase of ^{23}Na IR signal and a consecutive muscle weakness of the leg with provocation in all patients. Two patients developed complete paralysis of the upper and lower extremities after the first MR imaging examination. The paralysis dissolved nearly completely within the following 45 minutes. These patients reported having experienced several episodes of subtotal paralysis triggered by rest without moving prior to this event. It is known that complete rest following heavy physical strain is a typical trigger for sudden, temporary paralysis (29). Our findings confirm this is true for patients with HyperPP (2).

In several Na^+ channelopathies, such as hypokalemic periodic paralysis, therapy with acetazolamide has been suggested (9). In the current study, four patients seemed to have benefited from this treatment, as muscle edema decreased while muscle strength increased concomitantly. The results of our study indicate that acetazolamide may be a promising permanent medication for HyperPP to prevent irreversible muscle weakness. Further prospective studies will be needed to verify this hypothesis.

The absolutely low number of subjects may appear as a limitation of this study, but HyperPP is a rare disease (occurring in one of 200 000 persons), which makes recruiting a large number of subjects challenging. A further limitation is that the calculated overall Na^+ concentration within muscle tissue was not proved through muscle biopsy. The preliminary nature of our findings, given the low number of subjects, must also be acknowledged as a limitation. Last, it has to be emphasized that, to date, it is not possible to measure intra- and extracellular ^{23}Na separately with MR imaging. The IR preparation enables weighting of the measurement toward intracellular ^{23}Na, but significant contributions from the extracellular pool cannot be excluded.

In conclusion, ^{23}Na MR imaging seems to depict increased myoplasmic Na^+ in patients with HyperPP with permanent muscle weakness. This technique provides an excellent noninvasive method to assess whether medication is indicated and to monitor its success in patients with HyperPP. For this purpose, the ^{23}Na IR sequence in combination with a ^{23}Na spin-density image contrast and additional ^{1}H MR imaging is superior.

Acknowledgments: We thank the patients for their participation. We are grateful to Dr R. Rüdel, Division of Neurophysiology, Ulm University, Ulm, Germany, for discussion. Dr Lehmann-Horn is Senior Research Professor for Neurosciences of the nonprofit Hertie Foundation (Frankfurt, Germany). We are also grateful to Dr Maya B. Wolf, Department of Diagnostic and Interventional Radiology, University Hospital of Heidelberg, Heidelberg, Germany, for linguistic support. Special thanks go to Dr Simone Braun, Department of Biostatistics, German Cancer Research Center, Heidelberg, Germany, for statistical support.

Disclosures of Potential Conflicts of Interest: E.A. No potential conflicts of interest to disclose. **A.M.N.** Financial activities related to the present article: institution received a grant from the German Federal Ministry of Education and Research (project DOT-MOBI; 01IB08002). Financial activities not related to the present article: received payment for lectures including service on speakers bureaus from Siemens Healthcare (Siemens 3rd UHF User Meeting, Minneapolis, 2011). Other relationships: none to disclose. **M.A.W.** No potential conflicts of interest to disclose. **K.J.** No potential conflicts of interest to disclose. **F.L.** No potential conflicts of interest to disclose.

References

1. Fontaine B. Periodic paralysis. Adv Genet 2008;63:3–23.
2. Lehmann-Horn F, Rüdel R, Jurkat-Rott K. Nondystrophic myotonias and periodic paralyses. In: Engel AG, Franzini-Armstrong C, eds. Myology. 3rd ed. New York, NY: McGraw Hill Professional, 2004; 1257–1300.
3. Fontaine B, Khurana TS, Hoffman EP, et al. Hyperkalemic periodic paralysis and the adult muscle sodium channel alpha-subunit gene. Science 1990;250(4983):1000–1002.
4. Jurkat-Rott K, Lehmann-Horn F. Muscle channelopathies and critical points in functional and genetic studies. J Clin Invest 2005;115(8):2000–2009.
5. Venance SL, Cannon SC, Fialho D, et al. The primary periodic paralyses: diagnosis, pathogenesis and treatment. Brain 2006;129(pt 1):8–17.
6. Jurkat-Rott K, Lehmann-Horn F. Genotype-phenotype correlation and therapeutic rationale in hyperkalemic periodic paralysis. Neurotherapeutics 2007;4(2):216–224.
7. Jurkat-Rott K, Holzherr B, Fauler M, Lehmann-Horn F. Sodium channelopathies of skeletal muscle result from gain or loss of function. Pflugers Arch 2010;460(2):239–248.
8. McArdle B. Familial periodic paralysis. Br Med Bull 1956;12(3):226–229.
9. Jurkat-Rott K, Weber MA, Fauler M, et al. K+-dependent paradoxical membrane depolarization and Na+ overload, major and reversible contributors to weakness by ion channel leaks. Proc Natl Acad Sci U S A 2009;106(10):4036–4041.
10. Lehmann-Horn F, Küther G, Ricker K, Grafe P, Ballanyi K, Rüdel R. Adynamia episodica hereditaria with myotonia: a non-inactivating sodium current and the effect of extracellular pH. Muscle Nerve 1987;10(4):363–374.
11. Weber MA, Nielles-Vallespin S, Essig M, Jurkat-Rott K, Kauczor HU, Lehmann-Horn F. Muscle Na+ channelopathies: MRI detects intracellular 23Na accumulation during episodic weakness. Neurology 2006;67(7):1151–1158.
12. Constantinides CD, Gillen JS, Boada FE, Pomper MG, Bottomley PA. Human skeletal muscle: sodium MR imaging and quantification-potential applications in exercise and disease. Radiology 2000;216(2):559–568.
13. Hilal SK, Maudsley AA, Ra JB, et al. In vivo NMR imaging of sodium-23 in the human head. J Comput Assist Tomogr 1985;9(1):1–7.
14. Parrish TB, Fieno DS, Fitzgerald SW, Judd RM. Theoretical basis for sodium and potassium MRI of the human heart at 1.5 T. Magn Reson Med 1997;38(4):653–661.
15. Nagel AM, Laun FB, Weber MA, Matthies C, Semmler W, Schad LR. Sodium MRI using a density-adapted 3D radial acquisition technique. Magn Reson Med 2009;62(6):1565–1573.
16. Weber MA, Nielles-Vallespin S, Huttner HB, et al. Evaluation of patients with paramyotonia at ^{23}Na MR imaging during cold-induced weakness. Radiology 2006;240(2):489–500.
17. Winter PM, Bansal N. TmDOTP(5-) as a (23)Na shift reagent for the subcutaneously implanted 9L gliosarcoma in rats. Magn Reson Med 2001;45(3):436–442.
18. Ouwerkerk R, Bleich KB, Gillen JS, Pomper MG, Bottomley PA. Tissue sodium

concentration in human brain tumors as measured with ^{23}Na MR imaging. Radiology 2003;227(2):529–537.

19. Stobbe R, Beaulieu C. In vivo sodium magnetic resonance imaging of the human brain using soft inversion recovery fluid attenuation. Magn Reson Med 2005;54(5):1305–1310.

20. Nagel AM, Amarteifio E, Lehmann-Horn F, et al. 3 Tesla sodium inversion recovery magnetic resonance imaging allows for improved visualization of intracellular sodium content changes in muscular channelopathies. Invest Radiol 2011;46(12):759–766.

21. Dyck PJ, Boes CJ, Mulder D, et al. History of standard scoring, notation, and summation of neuromuscular signs: a current survey and recommendation. J Peripher Nerv Syst 2005;10(2):158–173.

22. Nielles-Vallespin S, Weber MA, Bock M, et al. 3D radial projection technique with ultrashort echo times for sodium MRI: clinical applications in human brain and skeletal muscle. Magn Reson Med 2007;57(1):74–81.

23. Early RG, Carlson BR, Casner SW Jr. Measured specific gravity, predicted specific gravity and total body water relationships in normal young men. Int Z Angew Physiol 1970;28(2):79–85.

24. Bachmann G, Damian MS, Koch M, Schilling G, Fach B, Stöppler S. The clinical and genetic correlates of MRI findings in myotonic dystrophy. Neuroradiology 1996;38(7):629–635.

25. Vilin YY, Ruben PC. Slow inactivation in voltage-gated sodium channels: molecular substrates and contributions to channelopathies. Cell Biochem Biophys 2001;35(2):171–190.

26. Banasiak KJ, Burenkova O, Haddad GG. Activation of voltage-sensitive sodium channels during oxygen deprivation leads to apoptotic neuronal death. Neuroscience 2004;126(1):31–44.

27. Marden FA, Connolly AM, Siegel MJ, Rubin DA. Compositional analysis of muscle in boys with Duchenne muscular dystrophy using MR imaging. Skeletal Radiol 2005;34(3):140–148.

28. Weber MA, Nagel AM, Jurkat-Rott K, Lehmann-Horn F. Sodium (23Na) MRI detects elevated muscular sodium concentration in Duchenne muscular dystrophy. Neurology 2011;77(23):2017–2024.

29. Lehmann-Horn F, Jurkat-Rott K. Voltage-gated ion channels and hereditary disease. Physiol Rev 1999;79(4):1317–1372.